Superhard semiconducting C_3N_2 compounds predicted via first-principles calculations

Fubo Tian, Jinhua Wang, Zhi He, Yanming Ma, Liancheng Wang, Tian Cui,* Changbo Chen, Bingbing Liu, and Guangtian Zou

State Key Laboratory of Superhard Materials, Jilin University, Changchun 130012, People's Republic of China

(Received 4 July 2008; revised manuscript received 14 November 2008; published 23 December 2008)

In this paper we introduce the two compounds α-C_3N_2 and β-C_3N_2 with cubic symmetry, which are derived from a simple cubic carbon (C_{20}) reported recently. Our first-principles calculations show that both the solids are highly incompressible with high bulk modulus (380 and 343 GPa), large shear modulus G (365 and 368 GPa), great elastic constant C_{44} (327 and 329 GPa), and high Vickers hardness H_V (both are 86 GPa), respectively. Accordingly we come to a conclusion that both the C_3N_2 phases are potentially superhard semiconductor materials. From the electronic partial density of states, it is found that the superhard character of the two phases is mainly attributed to the strong covalent bond between C and N. The α-C_3N_2 is dynamically stable at pressures below 1.2 GPa but unstable above 1.2 GPa because an optical branch softens to zero at the Γ point. The α-C_3N_2 will transform into β-C_3N_2 at about 1.2 GPa which is energetically more stable. Both phonon-dispersion and elastic constant calculations at zero and high pressures show that this β-C_3N_2 remains mechanically and dynamically stable in a pressure range from 0 to at least 20 GPa.

DOI: 10.1103/PhysRevB.78.235431 PACS number(s): 62.20.D−, 71.15.Mb, 63.20.D−, 71.20.−b

In the past few decades, the fact that diamond and cubic boron nitride (c-BN) are superhard materials has been accepted; meanwhile, extensive experimental and theoretical efforts have been devoted to the search of new superhard materials,[1] particularly to the covalent compounds formed by B, C, and N,[2–5] such as C_3N_4, c-BC_2N, and c-B_4C_3. In 1989, Liu and Cohen[6,7] comprehensively discussed the hardness of the hypothetical carbon nitride β-C_3N_4. They reported that such covalent solids composed of carbon and nitrogen are excellent candidates for extraordinary hardness. Recently, the B-C-N ternary compounds have become a focus of attention in this field, which are reported to be potential candidates for superhard materials.

Among those covalent compounds, the C-N materials attract much attention[8–12] by boasting their bond which is slightly shorter than the C-C bond in diamond. Similarly we focus on this type of material exploration. Most researchers agree on the definition that "superhard" materials are those with Vickers hardness (H_V) higher than 40 GPa.[13] Various views of searching for new superhard materials have been developed and explored in recent years and currently. Most of the superhard materials are insulators or semiconductors.[14] For nonmetals, hardness increases with the bulk modulus,[15] and the bulk modulus generally gets higher with smaller bond lengths and stronger covalent directional bonds. Solid with large shear modulus is considered as a potential ultrahard or superhard material.[16–18] In recent years, a new method[19,20] based on *ab initio* approach for predicting intrinsic superhardness of ideal crystals has been presented.

Different combinations of boron, carbon, and nitrogen can be checked for the search of novel isoelectronic structures. For doing that, the following simple rule[12] must be obeyed:

$$pZ_V(\mathrm{B}) + mZ_V(\mathrm{C}) + lZ_V(\mathrm{N}) = 4n. \quad (1)$$

The values p, m, l, and n are integers, and Z_V(B), Z_V(C), and Z_V(N) are the atomic valence states ($2s$ and $2p$) for boron, carbon, and nitrogen, respectively. Examples are represented by the systems BN, C_3N_4, $C_{11}N_4$, BC_2N, etc. In the present work, we focus our attention on C_3N_2 and manage to attain it by replacing part of the carbon atoms in simple cubic C_{20} (sc-C_{20}) with nitrogen atoms. Also, the C_3N_2 stoichiometry also corresponds to the above equation (1). The sc-C_{20} with Pm-3m space-group symmetry is shown in Fig. 1(a).[5] This structure is composed of 12 and 8 atoms in the 12j (labeled with 1) and 8g (labeled with 2) Wyckoff positions, respectively. As shown in Fig. 1, α-C_3N_2 is obtained from sc-C_{20} by substituting eight carbon atoms with eight nitrogen atoms in the 8g Wyckoff positions and remains the same space group as sc-C_{20}. The β-C_3N_2 structure is found to be the high-pressure phase of α-C_3N_2 with P-43m space-group symmetry and has 12 carbon atoms in the 12i and 8 nitrogen atoms in the 4e Wyckoff positions.

The present calculations are performed with CASTEP code based on the density-functional theory.[21] Both the generalized gradient approximation–Perdew-Burke-Ernzerhof

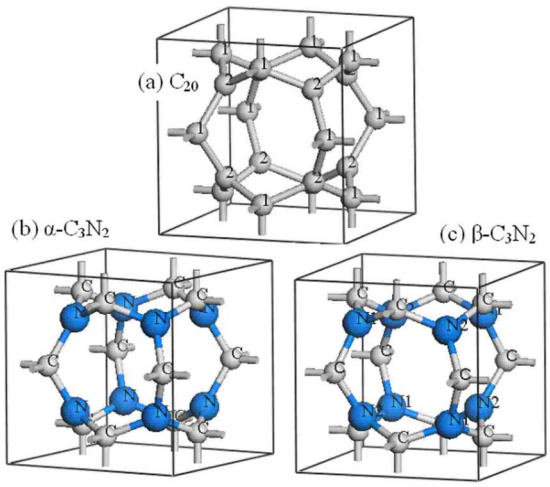

FIG. 1. (Color online) Unit cells of the simple cubic (a) C_{20} with the Pm-3m space group, (b) α-C_3N_2 with the Pm-3m space group, and (c) β-C_3N_2 with the P-43m space group. Carbon and nitrogen are depicted in gray and blue colors, respectively.

TABLE I. Equilibrium lattice parameters (in Å), Wyckoff positions, and nearest-neighbor (NN) distances.

	Cell constants (Å)	Wyckoff positions (r/a)	NN distances (Å)
C_{20}	5.152	C1(0.152,0.152,0.500)	$d_{C1\text{-}C1}=1.563$
		C2(0.263,0.263,0.263)	$d_{C1\text{-}C2}=1.466$
α-C_3N_2	5.054	C(0.155,0.155,0.500)	$d_{C\text{-}C}=1.569$
		N(0.257,0.257,0.257)	$d_{C\text{-}N}=1.427$
β-C_3N_2	5.049	C(0.155,0.155,0.497)	$d_{C\text{-}C}=1.568$
		N1(0.248,0.248,0.248)	$d_{C\text{-}N1}=1.422$
		N2(0.733,0.733,0.733)	$d_{C\text{-}N2}=1.433$

(GGA-PBE) (Ref. 22) and the local-density approximation–Ceperley-Alder-Perdew-Zunger (LDA-CAPZ) (Refs. 23 and 24) approaches of exchange-correlation functional were employed. We laid more stress on the results from the GGA and compared them with the ones from the LDA. The norm-conserving pseudopotential[25] with cutoff energy of 860 eV was used. According to Monkhorst-Pack scheme,[26] the k points of $8\times8\times8$ were used. The Mulliken overlap populations were integrated by a distance cutoff of 3 Å. The optimization of the lattice parameters and the ions relaxation were performed iteratively until the minimum of the total energy was met. The optimized parameters for C_{20} and C_3N_2, within the LDA and the GGA, are listed in Table I. It is clear that the predicted lattice parameters are larger with the GGA method than those with the LDA method, as in usual cases. To calculate the phonon-dispersion curve, the QUANTUM-ESPRESSO package,[27] with the density-functional perturbation theory,[28,29] was used.

In order to check the stability of α-C_3N_2, the elastic constants and phonon frequencies have been computed. The elastic stability is a necessary condition for a crystal to exist. A cubic stable crystal should obey the restrictions for its elastic constants[30,31]

$$C_{11}+2C_{12}>0,\ \ C_{44}>0,\ \ \text{and}\ \ C_{11}-C_{12}>0, \qquad (2)$$

where C_{11}, C_{12}, and C_{44} are the elastic stiffness constants. They can be deduced from the resulting change in the total energy by applying small strains to the equilibrium lattice. For a cubic crystal under hydrostatic pressure, the generalized elastic stability criteria[32,33] in analogy to the conventional criteria [Eq. (2)] are

$$c_{11}+2c_{12}>0,\ \ c_{44}>0,\ \ \text{and}\ \ c_{11}-c_{12}>0. \qquad (3)$$

In the case of hydrostatic pressure, the c_{ij} (in Voigt notation) are related to the C_{ij} defined with respect to the Eulerian strain variables by

$$c_{11}=C_{11},\ \ c_{12}=C_{12}+P,\ \ \text{and}\ \ c_{44}=C_{44}-P/2. \qquad (4)$$

Figure 2 shows the calculated elastic constants of α-C_3N_2 as functions of pressure. Obviously, c_{ij} fulfills the stability criteria stated above, suggesting that the structure is mechanically stable in a pressure range from 0 to at least 20 GPa. The phonon-dispersion curves for α-C_3N_2 at zero pressure are shown in Fig. 3. No imaginary phonon frequency was observed in the whole Brillouin zone (BZ), indicating that the α-C_3N_2 structure is dynamically stable at ambient pressure but is unstable at 1.2 GPa because an optical branch (dotted line in Fig. 3) softens to zero at the Γ point, while above this pressure imaginary phonon frequency was observed. Based on the eigenvectors of this softened mode, we distorted the original α-C_3N_2 to find the appropriate atomic displacements. After full geometry optimizations starting from the distorted structure, we got a structure with P-43m space-group symmetry called β-C_3N_2. The calculated elastic constants of β-C_3N_2 as functions of pressure are also shown in

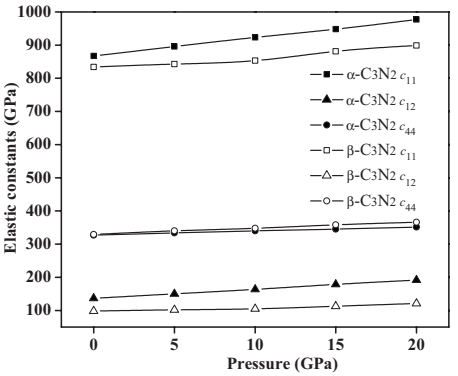

FIG. 2. Calculated elastic constants of c_{11}, c_{12}, and c_{44} for α-C_3N_2 (solid symbols) and β-C_3N_2 (open symbols) with pressure.

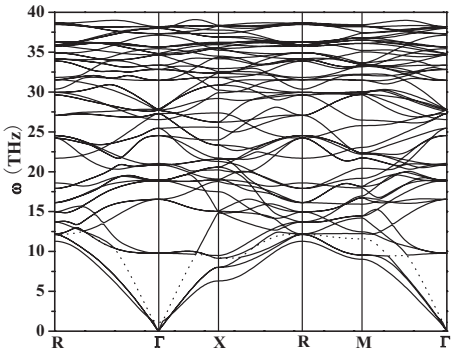

FIG. 3. The phonon-dispersion curves for the α-C_3N_2 configuration at ambient pressure.

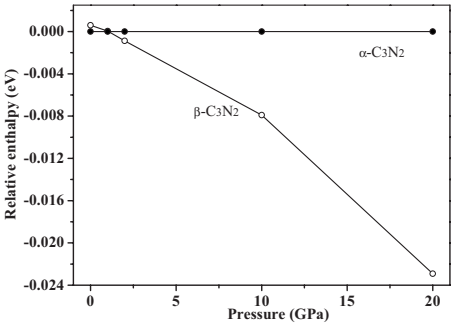

FIG. 4. Relative enthalpy (per f.u.) between α-C_3N_2 (solid symbols) and β-C_3N_2 (open symbols) as a function of pressure within the GGA level.

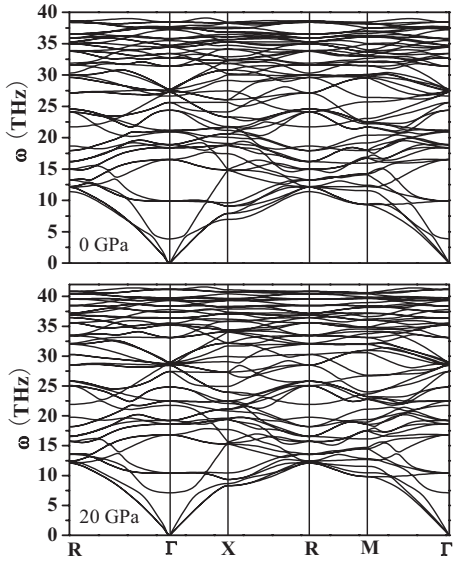

FIG. 5. The phonon-dispersion curves for the β-C_3N_2 at 0 and 20 GPa.

Fig. 2, indicating that the structure is mechanically stable in the pressure range from 0 to at least 20 GPa. In Fig. 4, the differences of the enthalpies between α and β phases are depicted. We found that β-C_3N_2 phase becomes energetically more favorable above 1.0 GPa. This transition pressure is well consistent with the result from the above phonon calculations. To further check the dynamical stability of β-C_3N_2, we calculated its phonon-dispersion curves, as shown in Fig. 5. It is clear that no imaginary phonon frequency exists in the whole BZ, indicating the dynamical stability of the β-C_3N_2 in a pressure range from 0 to at least 20 GPa.

To study the thermodynamic stability of both C_3N_2 materials, the formation enthalpy $\Delta H_f^{T=0}$ is calculated as

$$\Delta H_f^{T=0} = E_{\text{tot}}^{C_3N_2} - 3E_{\text{tot}}^{C} - E_{\text{tot}}^{N_2}, \tag{5}$$

where $E_{\text{tot}}^{C_3N_2}$ is the total energy of α- or β-C_3N_2 bulk, E_{tot}^{C} is the total energy of C taken from pure diamond, and $E_{\text{tot}}^{N_2}$ is the total energy of N from an early reported stable structure for a solid-state molecular form of nitrogen.[34] The calculated

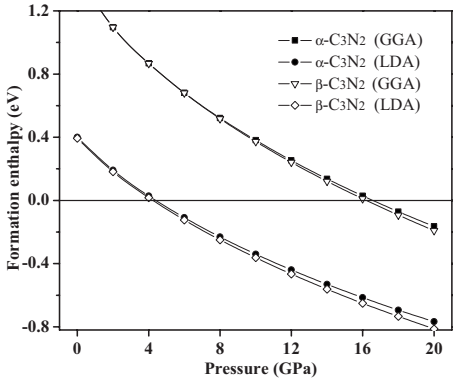

FIG. 6. The formation enthalpies of α-C_3N_2 (solid symbols) and β-C_3N_2 (open symbols) as functions of pressure within the GGA and LDA levels.

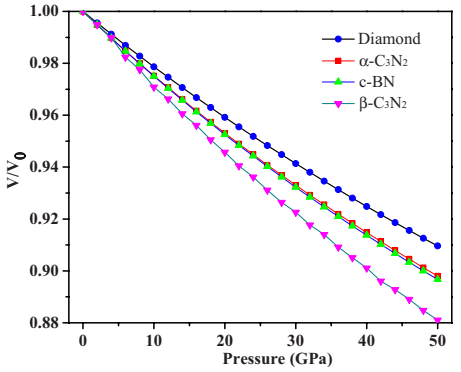

FIG. 7. (Color online) Calculated P-V relations for simple cubic α-C_3N_2 and β-C_3N_2 compared with those of diamond and cubic boron nitride.

formation enthalpies of α-C_3N_2 and β-C_3N_2 as functions of pressure within the LDA and the GGA are shown in Fig. 6. Indeed, we find that the GGA lowers the atomic total energies of C and N more than the solid C_3N_2. So the formation enthalpy within the GGA is higher than that within the LDA under the same pressure. The formation enthalpies suggest that both C_3N_2 phases are thermodynamically unstable at zero pressure because of their positive values. Thermodynamically stable phases are observed at above about 5.0 and 18.0 GPa within the LDA and the GGA, respectively.

The P-V relations [equation of state (EOS)] of α-C_3N_2, β-C_3N_2, diamond, and cubic boron nitride are given in Fig. 7 and show significantly different compression behaviors for the two closely related structures. The α-C_3N_2 is a highly incompressible solid and is more incompressible than c-BN and is resistant to shape deformation, which is an essential factor for hardness. However, the β-C_3N_2 can easily be compressed among the four structures. In order to gain a deeper insight into the hardness of the C_3N_2 materials, we calculate the band structures and density of states (DOS) of α-C_3N_2

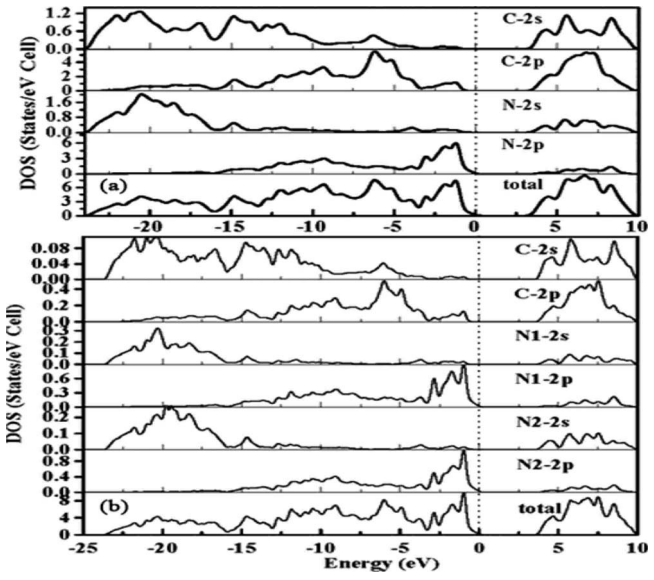

FIG. 8. Total and partial densities of states (DOSs) (a) for α-C_3N_2 and (b) for β-C_3N_2. The Fermi energy level is at zero.

TABLE II. The elastic stiffness constants C_{ij}, bulk modulus B, shear modulus G, Young's modulus E, Poisson's ratio ν, and B/G ratio of the simple cubic C_{20}, α-C_3N_2 and β-C_3N_2, compared with available experimental data for diamond and c-BN. All elastic constants except ν are in gigapascals.

	Method	C_{11}	C_{12}	C_{44}	B	E	G	ν	G/B
C_{20}	GGA	561	227	272	338	430	167	0.287	0.49
	LDA	550	245	256	347	400	153	0.307	0.44
α-C_3N_2	GGA	867	137	327	380	829	365	0.136	0.96
	LDA	880	149	327	393	838	366	0.145	0.93
β-C_3N_2	GGA	834	98	329	343	813	368	0.105	1.07
	LDA	830	100	334	343	808	365	0.107	1.06
c-BN	GGA	805	161	458	376	751	322	0.166	0.86
	LDA	806	176	466	386	743	315	0.179	0.82
	Expt.[a]	820	190	480	400	749	315	0.188	0.79
Diamond	GGA	1099	119	588	445	1075	490	0.097	1.10
	LDA	1099	135	598	456	1068	481	0.110	1.05
	Expt.[b]	1076	125	577	442	1143	535	0.068	1.21

[a]Reference 35.
[b]Reference 36.

and β-C_3N_2 at zero pressure. The band structures are not shown here, and the corresponding DOS and the atom-resolved partial density of states (PDOS) are shown in Fig. 8. The calculated electronic properties of α-C_3N_2 and β-C_3N_2 indicate that they are semiconductors with direct GGA band gaps (E_g) of 3.45 and 3.70 eV, respectively, in contrast with the metallic behavior of C_{20}.[5] From the PDOS of both C_3N_2 phases, it is found that the lower part of the valence band (VB) consists mainly of 2s states from nitrogen and carbon atoms, whereas at the top of the VB, just below the Fermi energy (E_F), the N 2p states hybridize strongly with the C 2p states. This strong hybridization of N p and C p also indicates a strong covalent bond between N and C.

Table II lists the calculated elastic stiffness constants C_{ij}, polycrystalline shear modulus G, Young's modulus E, Poisson's ratio ν, and B/G ratio of the simple cubic C_{20} α-C_3N_2 and β-C_3N_2, compared with available experimental data of both diamond[35] and c-BN.[36] The bulk modulus of the α-C_3N_2 phase is higher than that of C_{20}, even higher than that of c-BN. Besides the bulk modulus, we mention that the shear modulus, Young's modulus, and Poisson's ratio are also meaningful for illustrating the hardness of the simple cubic C_3N_2 materials. The shear modulus of a material quantifies its resistance to shear deformation and is a better indicator of potential hardness for ionic and covalent materials.[37,38] Young's modulus E is defined as the ratio between stress and strain and is used to provide a measure of the stiffness of the solid; i.e., the larger the value of E the stiffer the material is. Poisson's ratio quantifies the stability of the crystal against shear. The polycrystalline shear modulus G, Yong's modulus E, and Poisson's ratio ν in this table are calculated by means of the single-crystal elastic constants and the Voigt-Reuss-Hill approximation method[39] and can be obtained by the following formulas:

$$G = (C_{11} - C_{12})/2, \quad E = 9BG/(3B + G),$$

$$\nu = (3B - 2G)/[2(3B + G)]. \tag{6}$$

By considering the bulk modulus as a measure of the average bond strength and shear modulus as a measure of the resistance to a change in bond angle by an external force, Tanaka *et al.*[40] proposed that G/B represents the relative directionality of the bonding in the material. The calculated ratios G/B for α-C_3N_2 and β-C_3N_2 (0.96 and 1.07) are both slightly larger than that of c-BN (0.86) and close to that of diamond (1.10) at the GGA level, which indicates that the directionality of the bonding in the C_3N_2 materials is strong. The relative orientation of the bonding in the materials also has an important effect on their hardness. It should be noted that covalent hard crystals such as C_3N_4 and $C_{11}N_4$ have larger G/B values ($G/B \approx 0.9-1.2$) because of the higher angular stiffness of the strong directional covalent bonds.[11] The larger values of E mean that α-C_3N_2 and β-C_3N_2 are rather stiff. Our calculated Poisson's ratios are given in Table II for α-C_3N_2 and β-C_3N_2 (0.136 and 0.105) and are both smaller than the value calculated for c-BN (0.166). The smaller values of Poisson's ratio indicate that the C_3N_2 materials are relatively stable against shear. Thus, the above results provide a clear indicator that α-C_3N_2 and β-C_3N_2 are potential candidates for superhard materials.

According to the microscopic model of hardness,[19] the Vickers hardness for the C_3N_2 crystalline can be calculated as follows:

$$H_V = [(H_V^{\text{C-C}})^{n_1}(H_V^{\text{C-N}})^{n_2}]^{1/(n_1+n_2)}, \tag{7}$$

In Eq. (7), n_j ($j=1,2$) is the number of corresponding chemical bonds in the unit cell and $H_V^{X\text{-}Y}$ are the hardness of the hypothetical binary compound composed of the X-Y bond and can be calculated as

$$H_V^{X\text{-}Y} = 350(N_e^{X\text{-}Y})^{2/3} e^{-1.191 f_i^{X\text{-}Y}} / (d^{X\text{-}Y})^{2.5}, \tag{8}$$

where $d^{X\text{-}Y}$ is the length of the X-Y bond, $N_e^{X\text{-}Y}$ is the valence electron density, and can be calculated by

TABLE III. Bond parameters and hardnesses of the α-C_3N_2 and β-C_3N_2 phases compared with the calculated results for diamond and c-BN.

	Method	Bond	n_j	d	Ne	P	f_i	H_V (GPa)	H (GPa)
α-C_3N_2	GGA	C-C	12	1.569	0.466	0.71	0	68.2	86.3
		C-N	24	1.427	0.825	0.79	0.223	97.1	
	LDA	C-C	12	1.568	0.468	0.71	0	68.5	87.5
		C-N	24	1.422	0.835	0.80	0.221	98.9	
β-C_3N_2	GGA	C-C	12	1.568	0.468	0.71	0	68.5	86.0
		C-N1	12	1.422	0.836	0.78	0.239	96.9	
		C-N2	12	1.433	0.817	0.79	0.223	95.4	
	LDA	C-C	12	1.565		0.71	0	69.8	87.0
		C-N1	12	1.416		0.78	0.252	97.5	
		C-N2	12	1.430		0.80	0.221	96.7	
c-BN	GGA	B-N	16	1.558	0.687	0.65	0.239	67.7	67.7
	LDA	B-N	16	1.554	0.692	0.65	0.239	68.4	68.4
Diamond	GGA	C-C	16	1.529	0.727	0.75	0	98.0	98.0
	LDA	C-C	16	1.526	0.731	0.75	0	98.8	98.8

$$N_e^{X\text{-}Y} = [Z_X/N_X + Z_Y/N_Y]\left[\sum_j N^j (d^j)^3\right] \Big/ [V(d^{X\text{-}Y})^3], \quad (9)$$

where Z_X and Z_Y are the valence electron numbers of the X and Y atoms, N_X and N_Y are the nearest coordination numbers of the X and Y atoms, V is the volume of the unit cell, N^j is the number of j bond in the unit cell, and $f_i^{X\text{-}Y}$ is the Phillips ionicity of the X-Y bond. According to the generalized ionicity scale,[20] the Phillips ionicity f_i (or $f_i^{X\text{-}Y}$) can be calculated as

$$f_i = (f_h)^{0.735} = [1 - \exp(-|P_c - P|/P)]^{0.735}, \quad (10)$$

where f_h is the population ionicity scale of a bond, P is the overlap population of the X-Y bond, and P_c is the overlap population of a pure covalent bond in the simple cubic C_{20}. The theoretical Vickers hardnesses of α-C_3N_2, β-C_3N_2, diamond, and cubic boron nitride are listed in Table III. Our calculated results show that both C_3N_2 phases (both are 86 GPa) are not harder than the hardest diamond (98 GPa) but harder than the second hardest cubic boron nitride (68 GPa). β-C_3N_2 has the same hardness as α-C_3N_2 and higher hardness than c-BN, which is in agreement with the fact that hardness of a material is not directly related to its bulk modulus.

In summary, we have presented a completely theoretical analysis of the structural, elastic, and electronic properties of α-C_3N_2 and β-C_3N_2 using first-principles method. The α-C_3N_2 is demonstrated to be dynamically stable at pressures below 1.2 GPa and unstable at 1.2 GPa due to an optical branch softening to zero at the Γ point, while above this pressure, imaginary phonon frequency was observed, which results in the phase transition from α-C_3N_2 to β-C_3N_2. Results of the differences of the enthalpies between α and β phases indicate that β-C_3N_2 phase becomes energetically more favorable above 1.0 GPa. The β-C_3N_2 remains mechanically and dynamically stable in a pressure range from 0 to at least 20 GPa. The Vickers hardnesses (both are 86 GPa) of the semiconductive α-C_3N_2 and β-C_3N_2 phases are calculated according to the microscopic hardness model. We conclude that α-C_3N_2 and β-C_3N_2 are superhard semiconductors with direct gaps of 3.45 and 3.70 eV, respectively.

This work was supported by the National Natural Science Foundation of China under Grants No. 10574053 and No. 10674053, the 2004 NCET and 2003 EYTP of MOE of China, the National Basic Research Program of China under Grants No. 2005CB724400 and No. 2001CB711201, the 2007 Cheung Kong Scholars Programme of China, the Cultivation Fund of the Key Scientific and Technical Innovation Project under Project No. 2004-295, and the Changjiang Scholar and Innovative Research Team in University under Project No. IRT0625.

*Author to whom correspondence should be addressed. cuitian@jlu.edu.cn

[1] J. M. Léger and J. Haines, Endeavour **21**, 121 (1997).
[2] M. L. Cohen, Science **261**, 307 (1993).
[3] R. Riedel, Adv. Mater. (Weinheim, Ger.) **4**, 759 (1992).
[4] D. M. Teter and R. J. Hemley, Science **271**, 53 (1996).
[5] F. J. Ribeiro, P. Tangney, S. G. Louie, and M. L. Cohen, Phys. Rev. B **74**, 172101 (2006).
[6] A. Y. Liu and M. L. Cohen, Science **245**, 841 (1989).
[7] A. Y. Liu and M. L. Cohen, Phys. Rev. B **41**, 10727 (1990).

[8] C. M. Sung and M. Sung, Mater. Chem. Phys. **43**, 1 (1996).
[9] D. M. Teter and M. J. Hemley, Science **271**, 53 (1996).
[10] Michel Côté and Marvin L. Cohen, Phys. Rev. B **55**, 5684 (1997).
[11] M. Mattesini and S. F. Matar, Phys. Rev. B **65**, 075110 (2002).
[12] S. F. Matar and M. Mattesini, C.R. Acad. Sci., Ser. IIc: Chim **4**, 255 (2001).
[13] S. Vepřek, A. Zeer, and R. Riedel, in *Handbook of Ceramic Hard Materials*, edited by R. Riedel (Wiley, Weinheim, 2000).
[14] J. Haines, J. M. Léger, and A. Atouf, J. Am. Ceram. Soc. **78**, 445 (1995).
[15] J. M. Leger, J. Haines, and B. Blanzat, J. Mater. Sci. Lett. **13**, 1688 (1994).
[16] J. Haines, J. M. Léger, and G. Bocquillon, Annu. Rev. Mater. Res. **31**, 1 (2001).
[17] P. F. McMillan, Nature Mater. **1**, 19 (2002).
[18] J. E. Lowther, MRS Bull. **28**, 189 (2003).
[19] F. M. Gao, J. L. He, E. Wu, S. M. Liu, D. L. Yu, D. C. Li, S. Y. Zhang, and Y. J. Tian, Phys. Rev. Lett. **91**, 015502 (2003).
[20] J. L. He, E. Wu, H. T. Wang, R. P. Liu, and Y. J. Tian, Phys. Rev. Lett. **94**, 015504 (2005).
[21] M. D. Segall, P. J. D. Lindan, M. J. Probert, C. J. Pickard, P. J. Hasnip, S. J. Clark, and M. C. Payne, J. Phys.: Condens. Matter **14**, 2717 (2002).
[22] J. P. Perdew, K. Burke, and M. Ernzerhof, Phys. Rev. Lett. **77**, 3865 (1996).
[23] D. M. Ceperley and B. J. Alder, Phys. Rev. Lett. **45**, 566 (1980).
[24] J. P. Perdew and A. Zunger, Phys. Rev. B **23**, 5048 (1981).
[25] J. S. Lin, A. Qteish, M. C. Payne, and V. Heine, Phys. Rev. B **47**, 4174 (1993).
[26] J. D. Pack and H. J. Monkhorst, Phys. Rev. B **16**, 1748 (1977).
[27] S. Baroni, A. Dal Corso, S. de Gironcoli, P. Giannozzi, C. Cavazzoni, G. Ballabio, S. Scandolo, G. Chiarotti, P. Focher, A. Pasquarello, K. Laasonen, A. Trave, R. Car, N. Marzari, and A. Kokalj, http://www.pwscf.org/
[28] S. Baroni, P. Giannozzi, and A. Testa, Phys. Rev. Lett. **58**, 1861 (1987).
[29] P. Giannozzi, S. de Gironcoli, P. Pavone, and S. Baroni, Phys. Rev. B **43**, 7231 (1991).
[30] M. Born and K. Huang, *Dynamical Theory of Crystal Lattices* (Clarendon, Oxford, 1956).
[31] J. F. Nye, *Physical Properties of Crystals* (Oxford University Press, Oxford, 1985).
[32] J. Wang, S. Yip, S. R. Phillpot, and D. Wolf, Phys. Rev. Lett. **71**, 4182 (1993).
[33] J. Wang, J. Li, S. Yip, S. Phillpot, and D. Wolf, Phys. Rev. B **52**, 12627 (1995).
[34] J. A. Venables and C. A. English, Acta Crystallogr., Sect. B: Struct. Crystallogr. Cryst. Chem. **30**, 929 (1974).
[35] M. Grimsditch, E. S. Zouboulis, and A. Polian, J. Appl. Phys. **76**, 832 (1994).
[36] M. H. Grimsditch and A. K. Ramdas, Phys. Rev. B **11**, 3139 (1975).
[37] D. M. Teter, MRS Bull. **23**, 22 (1998)
[38] J. M. Léger, P. Djemia, F. Ganot, J. Haines, A. S. Pereira, and J. A. H. da Jornada, Appl. Phys. Lett. **79**, 2169 (2001).
[39] R. Hill, Proc. Phys. Soc., London, Sect. A **65**, 349 (1952).
[40] K. Tanaka, K. Okamoto, H. Inui, Y. Minonishi, M. Yamaguchi, and M. Koiwa, Philos. Mag. A **73**, 1475 (1996).